ELSEVIER

Characterization of Rh-based catalysts with EPR, TPR, IR and XPS

Yi Wang, Zhen Song, Ding Ma, Hongyuan Luo, Dongbai Liang, Xinhe Bao *

State Key Laboratory of Catalysis, Dalian Institute of Chemical Physics, The Chinese Academy of Sciences, Dalian 116023, China

Abstract

Rh-based catalysts to be used for the synthesis of C_2-oxygenates from syngas were characterized with EPR, TPR, IR and XPS methods. The chemical state of the Mn component was extensively studied with EPR after in situ reduction and treatment with various probe molecules. The results indicated that on the Mn/SiO_2 catalyst, Mn can exist as isolated Mn^{2+} ions on the surface of SiO_2 through the formation of coordination compounds with surface hydroxyls and H_2O molecules as ligands. Thermal reduction of the Mn/SiO_2 catalyst resulted in the migration and accumulation of the Mn^{2+} ions. The results of TPR, IR, XPS were consistent with those of EPR, which indicated that on a $Rh–Mn/SiO_2$ catalyst, a Rh–Mn mixed oxide was formed, which stabilized the Rh^+ species. The formation of small clusters of the Rh–Mn mixed oxide inhibited deep reduction and accumulation of the Mn component, while at the same time increased the dispersion of the Rh component. As a promoter, Mn acts as an electron acceptor, while Li exhibits an electron-donation effect. The Li component can inhibit the formation of Rh–Mn mixed oxide and increase the concentration of Rh^0 on the surface of SiO_2. The existence of Li may also cause the tilted-adsorption form of CO on Rh, as well as the spillover of H_2 from Rh to the SiO_2 support. © 1999 Elsevier Science B.V. All rights reserved.

Keywords: Characterization; Rh; Catalyst; EPR; TPR; IR; XPS

1. Introduction

It is well known that Rh/SiO_2 catalyst can be used for the selective conversion of synthesis gas to C_2-oxygenated compounds such as ethanol, acetaldehyde and acetic acid [1]. Addition of promoters to the basic Rh/SiO_2 catalyst recipe have striking effects on activity and selectivity. Manganese has been widely reported to be used as a promoter of rhodium, increasing its catalytic activity and, in some cases, the selectivity toward C_2-oxygenates, such as ethanol and acetic acid [2–5]. Recently, Luo et al. [6,7] and Lin et al. [8] further improved the selectivity of a $Rh–Mn/SiO_2$ catalyst by the introduction of Li components.

The unexpectedly large effects of the promoters on the activity and selectivity of the Rh/SiO_2 catalyst result from the interactions among Rh component, promoters and reactants. The effect of Mn addition was studied by Wilson et al. [9] with EPR, who noted that MnO could not be reduced to the metallic state but was present as Mn^{2+} in the actual catalyst. Moreover, the pro-

---

* Corresponding author. Tel.: +86-411-4686637; Fax: +86-411-4694447; E-mail: xhbao@gingko.dlut.edu.cn

moter element was in close contact with the rhodium crystallites. They postulated that MnO forms a mixed oxide with an oxidized form of rhodium. The formation of a mixed oxide would decrease the rate of CO dissociation, thereby reducing the amount of carbon on the catalyst and effectively increasing the active metal surface area. Van den Berg et al. [4] investigated a Rh–Mn–Mo/SiO$_2$ catalyst and suggested that manganese and molybdenum oxides partly cover the surface of the rhodium crystallites, thereby forming a mixed oxide containing Me–O–Rh bonds, which cannot be completely reduced by treatment with hydrogen at 500°C. A possible role of this mixed oxide is to weaken CO chemisorption, thus increasing the surface concentration of hydrogen atoms. Sachtler and Ichikawa [10] ascribed the improved activity of a Rh/SiO$_2$ catalyst promoted by oxophilic metal promoters such as Mn, Zr, V and Ti to the formation of a tilted mode of CO adsorption on the Rh surface, which was evidenced by the red shift of IR stretching frequency of the bridge-chemisorbed CO in the presence of oxophilic metal promoters. Wang et al. [11] reported that the composite active site for the formation of C$_2$-oxygenates on a Rh–Mn/SiO$_2$ catalyst was (Rh$_x^0$Rh$_y^+$)–O–Mn^{2+}, where $x \gg y$, according to the results of XPS and EPR.

However, the chemical state and environment of Rh, Mn and Li, as well as the interactions among them, have not been well studied. The role of the support (SiO$_2$) on the catalytic activity is not so clear, either. Since Mn^{2+} is paramagnetic, EPR provides a sensitive tool for studying the characteristics of the Rh–Mn/SiO$_2$ catalyst. However, the EPR results reported previously were not obtained under in situ conditions. In the present study, Mn/SiO$_2$, Rh–Mn/SiO$_2$ and Rh–Mn–Li/SiO$_2$ catalysts were investigated by EPR with in situ reduction treatments, and the variation of chemical state of the Mn component and interactions among various components were discussed. The results were basically consistent with those of TPR, XPS and CO-adsorbed IR experiments.

2. Experimental

2.1. Catalyst preparation

Catalysts were prepared by the incipient wetness technique using RhCl$_3 \cdot x$H$_2$O, Mn(NO$_3$)$_2$ and LiNO$_3$ in aqueous solution. SiO$_2$ (20–40 mesh, BET area 200 m^2 g^{-1}, Haiyang Chemical Plant, China) was used as the support material. Impregnated catalysts were dried in air, followed by calcining at definite temperatures. The loading amount of active components is in wt.% with respect to the weight of SiO$_2$.

2.2. Characterization of the catalysts by EPR

All the EPR experiments were carried out at room temperature, using a JEOL ES-ED3X X-band spectrometer. The microwave frequency $\nu = 9.239$ GHz, power of microwave = 1 mW, and the range of scanning field is 2500–4500 G.

The catalysts studied were: 0.2% Mn/SiO$_2$, 1% Rh–0.2% Mn/SiO$_2$, 1% Mn/SiO$_2$, 1% Rh–1% Mn/SiO$_2$, 1% Rh–2% Mn/SiO$_2$, 1% Rh–1% Mn–0.5% Li/SiO$_2$, 1% MnO$_2$/SiO$_2$.

Before the EPR spectra were recorded, the catalysts were reduced with H$_2$ or treated with other probe molecules under various conditions. All the processes were completed on a self-made apparatus for in situ treatment of the catalysts. The apparatus consists of a gas flow section, a reactor section and an evacuation section. The gas flow section controls the flow of H$_2$ and other gases to the reactor. The catalyst pellets (200 mg, 20–40 mesh) were loaded on the bottom of the reactor, which was made from a sample tube for EPR detection (4 mm i.d., quartz). The treating gas was introduced through a glass capillary tube (1 mm i.d.), with the tip inserted into the bottom of the catalyst bed. The gas flowed through the catalyst bed upwards from the bottom, and then outflowed via a three-way valve (Whitey SS-42 × S6MM). When switching from one kind of gas to another, the remnant gas in the system was evacuated through a mechanical pump via the three-

way valve. The catalyst was heated by a self-made furnace and the temperature was controlled by a XMT type temperature controller. After the pretreatment, the reactor was transferred to the resonance cavity of the EPR spectrometer for detection. In order to make the transfer of the reactor conveniently, the gas flow section was connected with the reactor by a flexible tube made of polyethylene. Such a setup made the measurements more convenient, and most important, it was possible to detect the EPR signals of the catalysts under conditions approximating those of real reactions.

The results of this report were taken from three different series of experiments: (1) Mn/SiO$_2$ after reduction with H$_2$ under different temperatures (2) Rh–Mn/SiO$_2$ and Rh–Mn–Li/SiO$_2$ catalysts after reduction with H$_2$ at various temperatures and (3) Mn-containing catalysts after and in the course of treatment with various probe molecules.

2.3. Other characterization methods

In addition to the EPR technique, TPR, CO-adsorbed IR and XPS methods were also employed to characterize the Rh-based catalysts.

TPR experiments were carried out in a conventional setup connected with different gases for the pretreatment of the sample, with a gas chromatography as the H$_2$ detector. The catalyst (about 50 mg) was put in a tubular quartz reactor. The sample was reduced by a mixture of 5% hydrogen and 95% argon at different temperatures. A relatively low heating rate, 16 K min^{-1}, was used in these experiments to eliminate the possible artifacts resulting from gas diffusion in the catalyst.

The adsorption states of CO on 1% Rh/SiO$_2$, 1% Rh–1% Mn/SiO$_2$ and 1% Rh–1% Mn–0.5% Li/SiO$_2$ were investigated by IR spectroscopy. The catalysts were reduced in flowing H$_2$ at 623 K for 2 h and then cooled to 300 K in high vacuum (10^{-3} Pa). The IR spectra of the reduced catalysts were treated as the backgrounds. 3000 Pa of CO was introduced into the

IR absorption cell at room temperature for 20 min and then evacuated to high vacuum. The IR absorption spectra of the adsorbed CO on the three catalysts were finally obtained by subtraction of the respective background spectra from that of adsorbed CO.

XPS spectra were recorded by a VG ESCALAB MK-2 X-ray photoelectron spectrometer using Al-Kα (1486.6 eV) as the exciting source. Si2p = 103.4 eV (for SiO$_2$) as internal standard was used to correlate the values of the obtained binding energy to normalize the charging effects appearing commonly on such non-conductive samples. In experiments, the samples were pressed into self-supported wafers and mounted on the stainless-steel manipulator. Base pressure of the system was 2×10^{-8} Pa. Samples utilized were: 1% Rh/SiO$_2$, 1% Rh–1% Mn/SiO$_2$ and 1% Rh–2% Mn–0.15% Li/SiO$_2$.

3. Results

3.1. Results of EPR experiments

The EPR spectra taken from Mn/SiO$_2$ samples with different Mn contents before and after reduction were plotted in Fig. 1. It can be seen that the two samples exposed in air at room temperature (RT) gave similar profiles of regular sextet features in the magnetic field range between 3000 and 3600 G, which are characteristic of isolated Mn^{2+} ions [9]. After being swept with H$_2$ at RT for 1 h, the intensities became much weaker, and they decreased continually with the increase of reduction temperature within the temperature range of RT–473 K. Above 473 K, the reduction resulted in broad peaks, which were assigned to Mn^{2+} ions produced through reduction, and dipole–dipole interactions among these ions were present [9]. The spectral variations of the two samples exhibited similar tendencies with the stepwise increase of the reduction temperature. We can see directly from the spectra that the amount of Mn^{2+} ions in the catalysts decreased firstly and
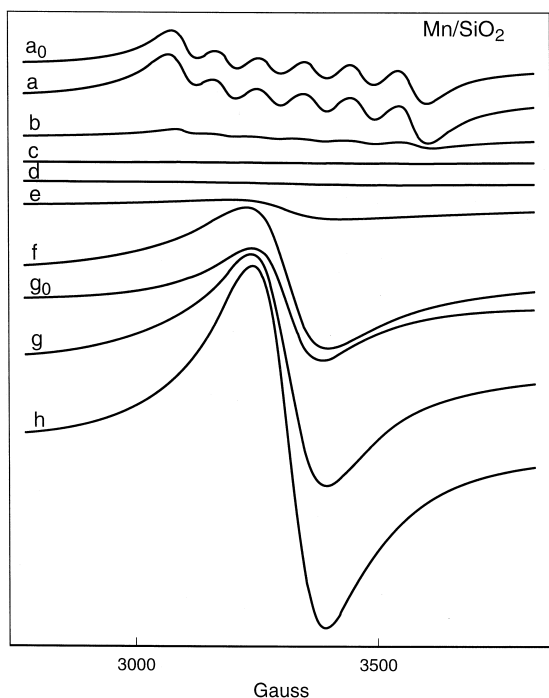
Fig. 1. EPR spectra of Mn/SiO_2 samples after reduction by H_2 at various temperatures for 1 h: (a_0) untreated 0.2% Mn/SiO_2; (a) untreated 1% Mn/SiO_2; (b)–(h) 1% Mn/SiO_2 after reduction at RT, 373 K, 473 K, 523 K, 573 K, 623 K and 673 K, respectively; (g_0) 0.2% Mn/SiO_2 after reduction at 623 K.

then increased following the increment of reduction temperature.

The situation was not the same when Rh and Li were added to the Mn/SiO_2 catalyst. Figs. 2 and 3 show the EPR spectra of the $Rh–Mn/SiO_2$ and $Rh–Mn–Li/SiO_2$ catalysts. Although the sextets could still be seen when exposing the $Rh–Mn/SiO_2$ catalyst in air, the spectra appeared to be distorted distinctly. The distortion, together with the intensive background of the observed spectra, reflected the presence of a certain amount of Mn^{2+} ions existing in an inhomogeneous magnetic environment. This may be due to interactions of Mn^{2+} with the Rh component [9]. After swept by H_2 at RT for 1 h, the intensity also became weaker, just as in the case of Fig. 1. However, when the reduction temperature reached 373 K, the broad peak appeared unambiguously. The pronounced low temperature for the appearance of the broad

Mn^{2+} signal indicates a strong interaction between the Rh and Mn components, which caused the reduction of Mn in high valence states (Mn^{3+}, Mn^{4+}) to Mn^{2+} more easily. On the other hand, the intensities of the broad peaks were almost unchanged with the increment of the reduction temperatures, which is very different from the case when pure Mn/SiO_2 samples were studied. This finding supports the previous inference that the existence of Rh inhibits deep reduction of the Mn component in the catalyst [4]. The Li component in the 1% Rh–1% Mn/SiO_2 catalyst weakened the interaction between Rh and Mn, as evidenced by the presence of a distinct sextet feature in the EPR spectrum obtained at room temperature (Fig. 3). Moreover, the Mn^{2+} ions appeared to be hardly produced by reduction at 373 K in the Li-promoted $Rh–Mn/SiO_2$ catalyst.
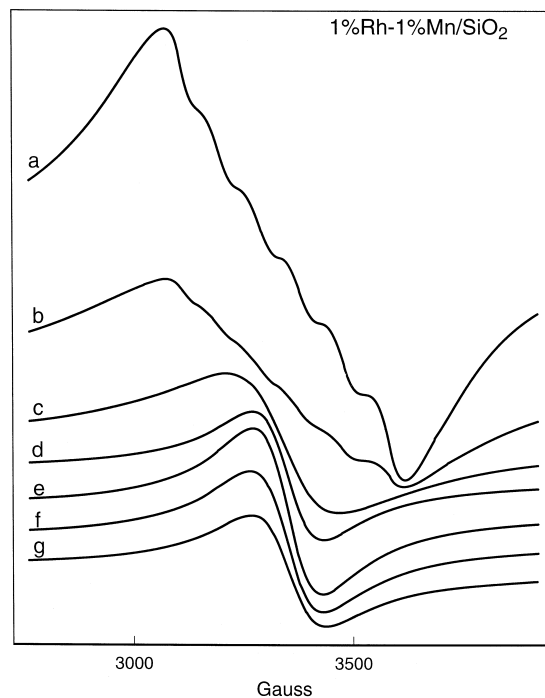

Fig. 2. EPR spectra of 1% Rh–1% Mn/SiO_2 after reduction by H_2 at various temperatures for 1 h: (a) untreated; (b)–(g) after reduction at RT, 373 K, 473 K, 523 K, 573 K and 623 K, respectively.
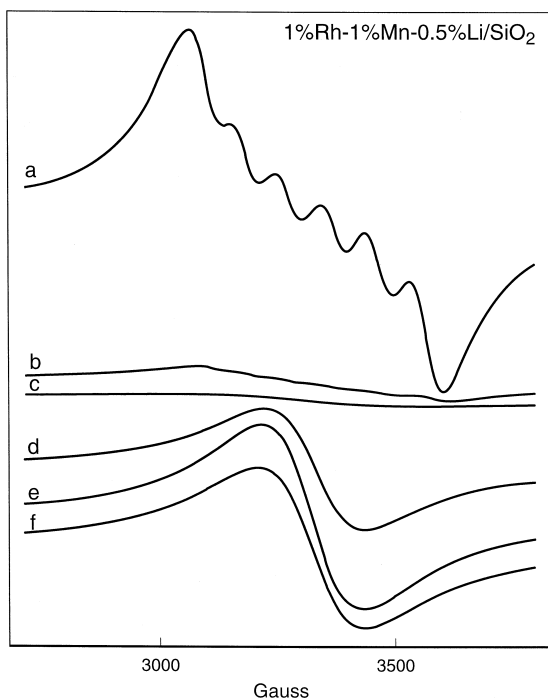
Fig. 3. EPR spectra of 1% Rh–1% Mn–0.5% Li/SiO$_2$ after reduction by H$_2$ at various temperatures for 1 h: (a) untreated; (b)–(f) after reduction at RT, 373 K, 473 K, 573 K and 623 K, respectively.

molecules as H$_2$O and C$_2$H$_5$OH can isolate the Mn^{2+} ions in the catalysts, and this effect is more prominent when H$_2$O is employed. Finally, in order to investigate the interaction between the Mn component and the surface of the SiO$_2$, a sample prepared by mechanically mixing MnO$_2$ powder with SiO$_2$ was also studied by EPR. The corresponding results were shown in Fig. 4c. It was found that no obvious peak characterizing Mn^{2+} ions was exhibited even after the sample was reduced at 573 K for 1 h (the small peaks at about 3300 G might be due to other paramagnetic centers in MnO$_2$). This result demonstrated that Mn^{2+} ions cannot exist in MnO$_2$ and the matrix of silica can supply an appropriate environment for accommodating the Mn^{2+} species.
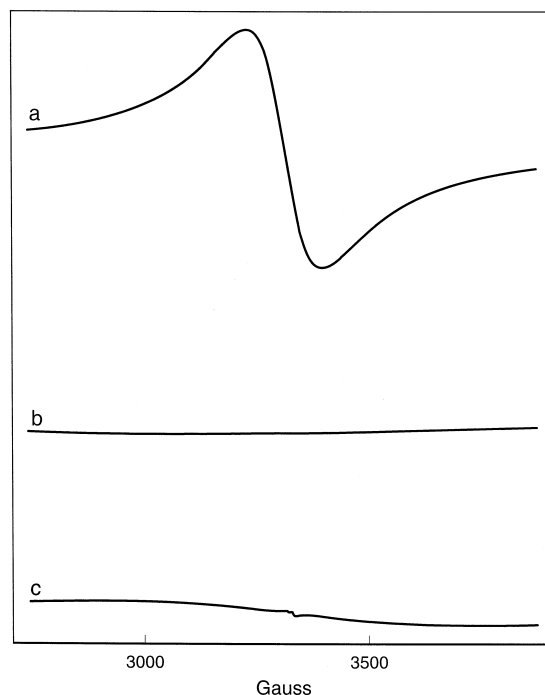
In order to ascertain the chemical state of the Mn species on the surface of silica, additional experiments were concentrated on the 1% Mn/SiO$_2$ sample under various treatments, as shown in Figs. 4 and 5. Fig. 4b showed the EPR spectra of 1% Mn/SiO$_2$ treated at 573 K by N$_2$, it is obvious that Mn^{2+} species was eliminated. To get some sense about the interaction of polar molecules with the Mn component, H$_2$O and C$_2$H$_5$OH were employed to treat the 1% Mn/SiO$_2$ after reduction at 623 K. Their introduction was carried out by bubbling H$_2$ through the liquid H$_2$O or C$_2$H$_5$OH at RT. After treating the sample with such polar molecules for a period of time, the hyperfine structure of sextets appeared from the broad peak background, and it became clearer with an increase of treating time. As H$_2$O and C$_2$H$_5$OH were swept off by H$_2$, the sextets disappeared again. So we concluded that such polar

Fig. 4. EPR spectra of 1% Mn/SiO$_2$ and MnO$_2$/SiO$_2$ after different treatments. (1) 1% Mn/SiO$_2$ after reduction with H$_2$ at 573 K for 1 h; (b) 1% Mn/SiO$_2$ after treating with N$_2$ at 573 K for 1 h; (c) MnO$_2$/SiO$_2$ (prepared by mechanically mixing MnO$_2$ powder with SiO$_2$) after reduction with H$_2$ at 573 K for 1 h.
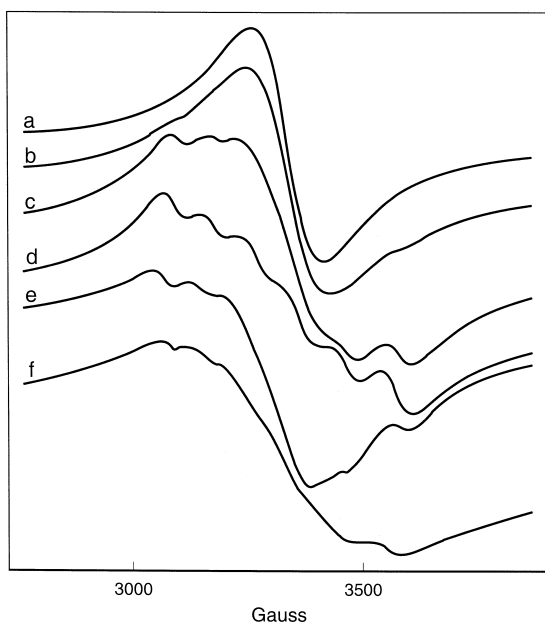
Fig. 5. EPR spectra of reduced 1% Mn/SiO_2 after treatment with H_2O or C_2H_5OH. (a) After reduction at 623 K; (b)–(d) the reduced sample after treating with H_2O for 8 min, 30 min and 60 min, respectively. (e), (d) After sweeping with H_2 to remove H_2O at RT overnight. (f) The reduced sample after treating with C_2H_5OH for 60 min.

3.2. Results of TPR, IR and XPS

Fig. 6 presents TPR profiles of various catalysts. It is found that reduction of Rh supported on SiO_2 started at about 370 K and reached its maximum at 420 K, while Mn on the same support was reduced at about 620 K. Addition of Mn to the Rh/SiO_2 led to a shift of the reduction peak of rhodium towards higher temperatures, while at the same time the reduction peak of the manganese component appeared at a lower temperature. These results show that the added manganese in the catalysts exhibited a suppression effect for the reduction of the rhodium precursor. Similar results have been reported by Luo et al. in their recent paper [12].

For the 1% Rh/SiO_2 catalyst, the addition of a small amount of Li increased the hydrogen consumption pronouncedly, and the temperature for Rh reduction shifted remarkably from 420 K to 570 K (curve e). Curve (f) in Fig. 6 presents

the TPR spectrum taken from the 1% Rh–2% Mn/SiO_2 catalyst promoted by 0.5% Li. Comparing with the spectrum taken from 'pure' $Rh-Mn/SiO_2$, it appears rather remarkable that the maximum of the reduction peak shifted from 450 K to 570 K and, moreover, the peak split into two obvious uptakes with a temperature difference of 30 K. In fact, the optimal yield of C_2-oxygenates was obtained at about 570 K on the $Rh-Mn-Li/SiO_2$ catalyst [8]. Although it seems to be too early to draw some conclusions for the function of lithium in the catalysts, it is quite clear that the Li component, serving as a promoter, can regulate the reduction temperature of the rhodium in the catalysts, and there is the possibility that the Li component can induce a spillover effect of H_2 to the support (SiO_2) so as to increase the H_2 consumption pronouncedly.

The IR spectra taken respectively from 1% Rh/SiO_2, 1% Rh–1% Mn/SiO_2 and 1% Rh–1% Mn–0.5% Li/SiO_2 after adsorption of CO were shown in Fig. 7. According to Yang and
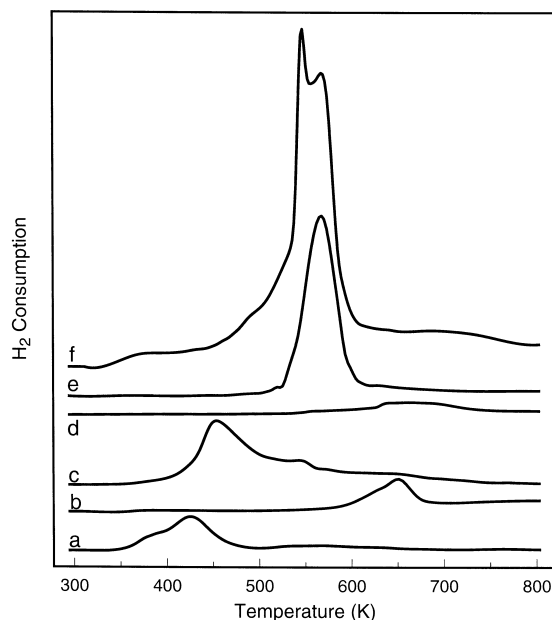

Fig. 6. TPR profiles of various catalysts. (a) 1% Rh/SiO_2, (b) 1% Mn/SiO_2, (c) 1% Rh–1% Mn/SiO_2, (d) 0.15% Li/SiO_2, (e) 1% Rh–0.15% Li/SiO_2, (f) 1% Rh–2% Mn–0.5% Li/SiO_2.
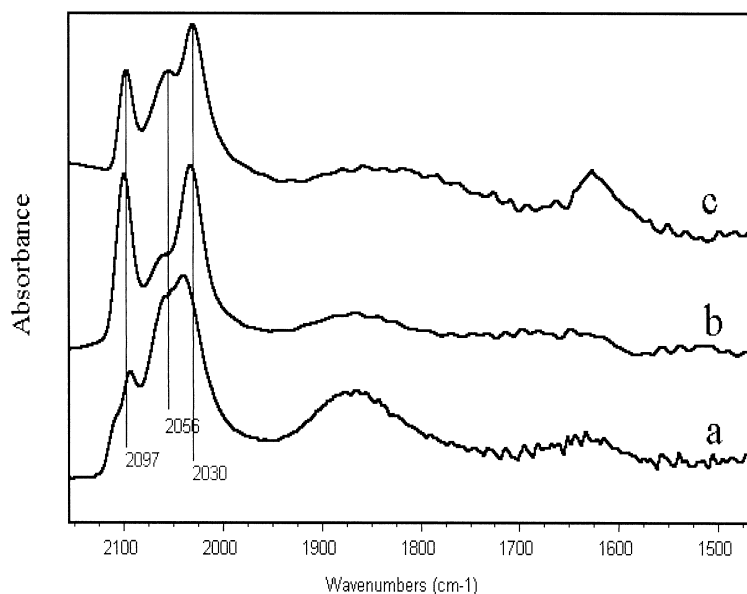
Fig. 7. CO-adsorbed IR spectra of Rh-based catalysts. (a) 1% Rh/SiO_2, (b) 1% $Rh–1\%$ Mn/SiO_2, (c) 1% $Rh–1\%$ $Mn–0.5\%$ Li/SiO_2.

Garland [13], the broad bands in the range of 1800–1900 cm^{-1} were ascribed to CO adsorbed on the bridge sites of Rh (bridged form adsorption); the bands at about 2057 cm^{-1} were ascribed to the CO adsorbed on the top sites of Rh (linear form adsorption); the double bands centered at 2010 and 2032 cm^{-1}, respectively were due to the geminal adsorption state of CO on top of Rh (geminal form adsorption); and the broad bands near 1635 cm^{-1} might result from a kind of tilted adsorbed CO with the C on the bridge sites of Rh and the O on Mn.

As shown in Fig. 7, the IR absorptions of CO in linear and bridged adsorption states on the Rh/SiO_2 catalyst were the strongest among the three catalysts, and CO existed mainly in the linear form. After adding Mn as a promoter, the intensities of linear and bridged forms decreased, whereas the geminal form became the major adsorption state of CO on the catalyst. On the $Rh–Mn–Li/SiO_2$ catalyst, the intensity of the linear form of CO increased pronouncedly in comparison with that on the catalyst containing only Mn as the promoter.

The results of XPS experiments were shown in Fig. 8. It is known that BEs of Rh^0, Rh^+ and

Rh^{3+} are 307.1 eV, 307.6–309.6 eV and 308.8–311.3 eV, respectively [14,15]. Curve (a) indicated that the $Rh3d_{5/2}$ peak taken from the Rh/SiO_2 catalyst appeared to be centered at about 308.0 eV. This reflected that the Rh component in this catalyst existed in a non-stoichiometric state, which was between metallic Rh and Rh_2O_3. The addition of Mn enhanced the oxidation state of Rh in the catalyst to give rise to a full-oxidized Rh species (Rh_2O_3), as evidenced by the shift of the binding energy of $Rh3d_{5/2}$ towards higher energies. Further addition of Li to the system led to a dramatic change of the state of the Rh species. As shown in curve (c), the Rh3d spectrum taken from the 1% $Rh–2\%$ $Mn–0.5\%$ Li/SiO_2 catalyst split into two groups, and an uptake representing metallic Rh emerged at about 306.8 eV, while the dominant peak of $Rh3d_{5/2}$ showed a 0.5 eV shift towards higher energy with respect to the value obtained from the 1% $Rh–1\%$ Mn/SiO_2. This result reveals that Li as a promoter in the catalyst served as an electron donor, and its interaction with the surface of Rh induced apparently the reduction of the surrounded Rh atoms. Other Rh atoms uncon-
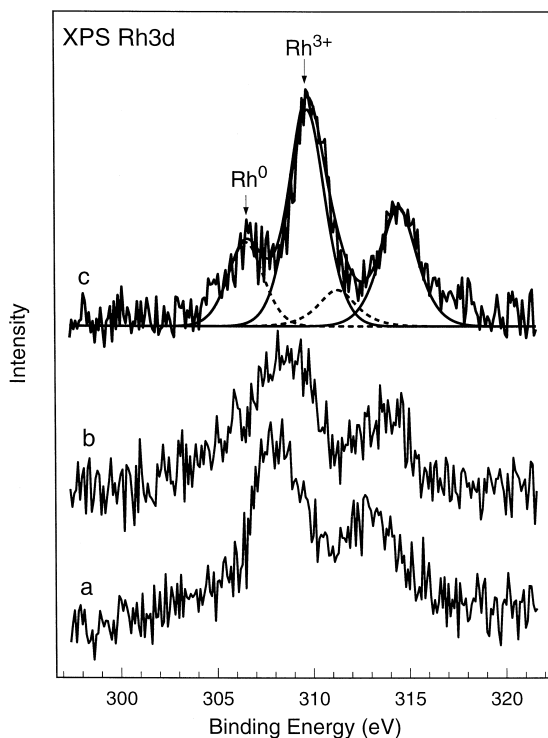
Fig. 8. XPS spectra of Rh-based catalysts. (a) 1% Rh/SiO_2, (b) 1% Rh–1% Mn/SiO_2, (c) 1% Rh–2% Mn–0.5% Li/SiO_2.

nected with Li atoms showed a more positive property with respect to the stoichiometric Rh_2O_3. The ratio of the spectral intensities of the two different Rh species on the catalyst surface is about 0.5, which refers to the amount of Li atoms in the system and seems to imply some correlation between the Li atoms and the Rh atoms in the catalyst.

4. Discussion

The present EPR results show that the reduction conditions affect the Mn component in two important ways. Firstly, the coordination states of the Mn^{2+} ions were changed, and secondly, the valence state of the Mn component varied as well. The existence of isolated Mn^{2+} in the catalysts exposed in air might be due to the adsorption of water, as confirmed by the results described in Fig. 5. In fact, all the EPR spectra

of the Mn/SiO_2 samples exposed in air at RT were very similar to that of Mn^{2+} ions in aqueous solutions [16]. It is well known that Mn^{2+} exists as hydrous ions with a structure of $[Mn(H_2O)_6]^{2+}$ in aqueous solutions, which is stable under neutral and acidic environments [17]. In the present Mn/SiO_2 system, a stable coordination compound of Mn^{2+} might form with H_2O and surface hydroxyls as ligands. It is reported [18] that during preparation of a heterogeneous catalyst with transition metal ions as active component and with an oxide as support, the surface of the oxide exerts a chelating effect to the transition metal ions to form a surface *cis*-octahedral complex in the liquid–solid interfaces, where the oxide surface supplies a supramolecular bidentate ligand via such as *vicinal* $\equiv SiO^-$ groups. This process is accompanied by an entropy increase. It is important to note that once the transition metal ions coming from complexes of the liquid phase become bonded to the oxide surface, they can remain attached to the support even though the liquid phase is eliminated and the remaining gas–solid system heated at higher temperatures. It is then possible to produce vacant coordination sites. The reactivity of such sites toward ligand addition or substitution is the driving force for adsorption and catalysis. According to the ideas stated above, we gave a model of formation of isolated Mn^{2+} species as shown in Fig. 9.

However, when swept by H_2 below 473 K, the adsorbed water will be removed from the surface of Mn/SiO_2 catalysts, resulting in the appearance of unsaturated coordinated Mn^{2+} ions on the surface of SiO_2. So the trace amount of oxygen or other oxidants in H_2 can attack the Mn^{2+} ions from the vacant coordination sites, and the Mn^{2+} species can be readily oxidized to higher valence states (Mn^{3+} and Mn^{4+}). In fact, there is a certain amount of higher valence state Mn on the as-synthesized Mn/SiO_2 catalysts, this can be seen from the color (pink) of the samples. The signal intensities of untreated 0.2% Mn/SiO_2 and 1% Mn/SiO_2 were not proportional to the content of the Mn component, this
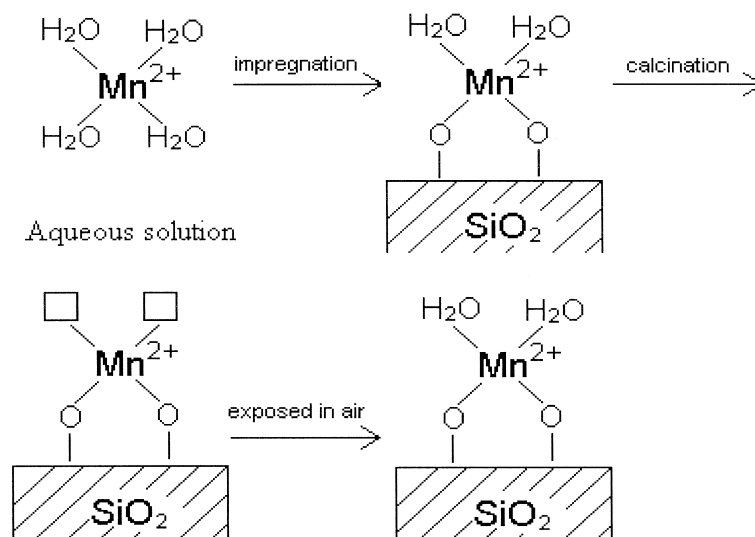
Fig. 9. The formation process of Mn^{2+} surface complex.

implied that the amount of isolated Mn^{2+} was determined by the number of surface hydroxyls on the support. Only those Mn^{2+} ions bonded with surface hydroxyls can exist stably.

The dipole–dipole interaction among Mn^{2+} ions after reduction was not simply due to the increase of Mn^{2+} concentration, as stated in the literature [12]. Because we found that the intensity of the broad peak was not always much larger than the sextet intensity before reduction, and it was even weaker than the latter when the reduction temperature was not high enough. Here we ascribe this phenomenon to the motion of the Mn^{2+} species on the support surface during the reduction process, and the driving force for this motion is the inclination to diminish the surface Gibbs free energy. We suggest that the reduced Mn^{2+} ions at elevated temperatures could overcome the potential hills to move into places where they could anchor more strongly on the surface. This process resulted in the accumulation of Mn^{2+} ions, so the dipole–dipole interactions between them strengthened as well. The accumulated Mn^{2+} ions connected with each other through Mn–O–Mn bonds and existed independent of the surface hydroxyls, so the concentrations were closely related to the

Mn contents of the catalysts, as evidenced by curves (g_0) and (g) in Fig. 1.

On the other hand, the addition of Rh to the Mn/SiO_2 catalyst caused the reduction of high valence state Mn to Mn^{2+} more easily, which is in agreement with the TPR results described above. This suggests that Rh and Mn oxides are in close proximity. Metallic rhodium provides sites for hydrogen adsorption and dissociation with extremely low activation energy. If MnO_x particles are close enough to metal sites, their reduction by atomic hydrogen takes place at a lower temperature than if molecular hydrogen has to interact with MnO_2, so the reducibility of higher Mn oxides is enhanced by the close proximity of Rh [19]. However, the inhibition effect of Rh for further reduction of Mn oxides can be interpreted by the formation of small clusters of mixed Rh and Mn oxide. Similar to Mn^{2+} ions, Rh species could move during reduction process, resulting in the formation of small clusters with Mn component in definite places on the support. So there existed two kinds of Mn species in the clusters, one was located on the surface of the cluster which was bonded with the surface of silica, the other lay inside the cluster connecting with other atoms

through Mn–O–Rh bonds. Only those Mn^{2+} ions bonded to the surface of SiO_2 can exist stably.

The formation of Rh–Mn mixed oxide was also confirmed by results of IR and XPS experiments. According to Ichikawa and Fukushima [20], CO adsorbed on Rh^+ centers was mainly in the geminal form, while on Rh^0 CO was adsorbed mainly in the linear form. Fig. 7 shows that on the Rh–Mn/SiO_2 catalyst, the concentration of Rh^+ was the highest among the three catalysts. From curve (b) in Fig. 8 the same conclusion could be drawn. Both the results indicated that the existence of the Mn component could stabilize the Rh^+ species. Because the geminally adsorbed CO requires isolated Rh^+ centers, so it implied that the dispersion of the Rh component was enhanced after the addition of Mn to the Rh/SiO_2 sample. On the other hand, both the XPS and IR results indicated that the existence of Li promoted the production of Rh^0 species on the surface of silica. So the amount of Rh oxide may be less in the 1% Rh–1% Mn–0.5% Li/SiO_2 than in the 1% Rh–1% Mn/SiO_2 catalyst, and consequently, the mixed oxide of Rh and Mn was more difficult to form in the former sample. The possible spillover effect of H_2 to the support induced by Li and its effect on the catalytic activity will be further investigated in the future.

5. Conclusions

(1) On the Mn/SiO_2 sample, isolated Mn^{2+} ions could exist stably on the surface of silica through formation of coordination compound with surface hydroxyls and H_2O molecules as ligands. The loss of H_2O resulted in the formation of unsaturated surface complex of Mn^{2+}, which could be readily oxidized to higher valence state by trace amount of O_2 under temperatures below 473 K. Thermal reduction of Mn/SiO_2 at elevated temperatures led to migration and accumulation of Mn^{2+} ions on the surface of SiO_2, so that the distances between these Mn^{2+} ions were shortened and the dipole–dipole interactions among them were strengthened. Such polar molecules as H_2O and C_2H_5OH could weaken these interactions and isolate the Mn^{2+} again. Only those Mn^{2+} ions bonded with surface hydroxyls could exist stably on the surface of SiO_2.

(2) The results of TPR, IR and XPS were consistent with those of EPR, indicating that on the Rh–Mn/SiO_2 catalyst, Rh–Mn mixed oxide was formed, which stabilized the existence of the Rh^+ species. The formation of small clusters of Rh–Mn mixed oxide inhibited deep reduction and accumulation of the Mn component, while at the same time, increased the dispersion of the Rh component. As a promoter, Mn acted as an electron acceptor, while Li exhibited an electron-donation effect. Li component could inhibit the formation of Rh–Mn mixed oxide and increase the concentration of Rh^0 on the surface of SiO_2. The existence of Li might also cause the tilted-adsorption form of CO on Rh, and the spillover of H_2 from Rh to the support (SiO_2).

Acknowledgements

References

[1] H. Arakawa, K. Takeuchi, T. Matsuzaki, Y. Sugi, Chem. Lett. (1984) 1607.
[2] P.C. Ellgen, W.J. Bartley, M.M. Bhasin, T.P. Wilson, Adv. Chem. Ser. 178 (1979) 147.
[3] H. Orita, S. Naito, K. Tamaru, J. Chem. Soc. Chem. Commun. (1984) 150.
[4] F.G.A. Van den Berg, J.H.E. Glezer, W.M.H. Sachtler, J. Catal. 93 (1985) 340.
[5] H. Trevino, W.M.H. Sachtler, Catal. Lett. 27 (1994) 251.
[6] H.Y. Luo, A.G.T.M. Bastein, A.A.J.P. Mulder, V. Ponec, Appl. Catal. 38 (1988) 241.
[7] H.Y. Luo, S.B. Xie, L.W. Lin, D.B. Liang, Chin. J. Catal. 16 (1995) 136.

[8] P.Z. Lin, D.B. Liang, H.Y. Luo, C.H. Xu, H.W. Zhou, S.Y. Huang, L.W. Lin, Appl. Catal., A 131 (1995) 207.

[9] T.P. Wilson, P.H. Kasai, P.C. Ellgen, J. Catal. 69 (1981) 193.

[10] W.M.H. Sachtler, M. Ichikawa, J. Phys. Chem. 90 (1986) 4752.

[11] H. Wang, J. Liu, J. Fu, K. Tsai, Chin. J. Mol. Catal. 7 (1993) 252.

[12] H.Y. Luo et al., J. Mol. Catal. A: Chem. 122 (1997) 115.

[13] A.C. Yang, C.W. Garland, J. Phys. Chem. 61 (1957) 1504.

[14] J.S. Brinen, A. Malera, J. Phys. Chem. 76 (1972) 2525.

[15] J.S. Brinen, A. Malera, J. Catal. 40 (1975) 295.

[16] Y. Xie, M. Shao, Structural Chemistry, Advanced Education, Beijing, 1991, p. 296.

[17] X. Cao, et al., Inorganic Chemistry, Advanced Education, Shanghai, 1987, p. 439.

[18] K. Dyrek, M. Che, Chem. Rev. 97 (1997) 305.

[19] H. Trevino et al., J. Catal. 154 (1995) 245.

[20] M. Ichikawa, T. Fukushima, J. Phys. Chem. 89 (1985) 1564.